Available online at www.sciencedirect.com
SCIENCE DIRECT®
Engineering Structures 27 (2005) 431–441
ENGINEERING STRUCTURES
www.elsevier.com/locate/engstruct

Short time Fourier transform algorithm for wind response control of buildings with variable stiffness TMD

Satish Nagarajaiah*, Nadathur Varadarajan

Department of Civil and Env. Eng. and Mech. Eng. and Mat. Sc., MS318, Rice University, Houston, TX 77005, United States

Received 31 December 2003; received in revised form 1 October 2004; accepted 29 October 2004
Available online 22 December 2004

Abstract

The new semi-active variable stiffness tuned mass damper (SAIVS-TMD) system, developed by the authors, is capable of continuously varying its stiffness and retuning its frequency in real time. The tuned mass damper (TMD) system can only be tuned to a fixed frequency, which is the first mode frequency of the building. The SAIVS-TMD system is robust to changes in building stiffness and damping.

The short time Fourier transform (STFT) is the most widely used method for studying non-stationary signals. The basic idea of short time Fourier transform is to break up the signal into small time segments and Fourier analyze each time segment to ascertain the frequencies that exist in it. For each different time a different spectrum is obtained and the totality of these spectra is the time–frequency distribution. The new idea proposed in this study is to use STFT to identify the dominant frequency of response, and track its variation as a function of time to retune the SAIVS-TMD.

The effectiveness of a SAIVS-TMD controlled by the new STFT algorithm for response reduction of a wind excited tall building is investigated in this study. An analytical model of the tall building with time varying stiffness of SAIVS-TMD is developed. The frequency tuning of the SAIVS-TMD is achieved by a new time frequency algorithm based on STFT. It is shown that the SAIVS-TMD can reduce the structural response, when compared to the uncontrolled case and the case with TMD. SAIVS-TMD is particularly effective in reducing the response when the building stiffness changes; the TMD loses its effectiveness under building stiffness variations. The response reductions due to an active tuned mass damper can also be achieved by SAIVS-TMD—with an order of magnitude less power consumption—with the STFT algorithm.

Keywords: Short time Fourier transform; Real time tuning; Variable stiffness device; Smart tuned mass damper; Semiactive structural control; Wind excitation

1. Introduction

The variation in stiffness or damping of the system is used to control the response in semi-active control systems as compared to direct application of control force in fully active systems. Variable stiffness and damping systems have been investigated by several researchers [5,8,10,11,13,18–20,26]. A new semi-active continuously and independently variable stiffness (SAIVS) device has been developed by Nagarajaiah [14]. Effectiveness of tuned mass dampers (TMD) [4] and multiple tuned mass dampers (MTMD) [7] has been studied widely. TMD are very sensitive to tuning frequency ratio, even when optimally designed [4,23]. Such a limitation of the TMD can be overcome by a MTMD [7] with the natural frequencies of a large number of small TMD's distributed around the fundamental natural frequency of the structure. Several researchers have studied active tuned mass dampers (ATMD) [2,17] and active mass dampers (AMD) [9,17]. ATMD and AMD's have been implemented in several real buildings [9,16,17,19]. An extensive survey of semi-active tuned vibration absorbers has been presented by Sun et al. [21]. Semi-active TMD for structural control has been proposed by Hrovat et al., Abe and Igusa and Yalla et al. [6,1,24].

Semi-active variable stiffness tuned mass damper (SAIVS-TMD) has been developed by Nagarajaiah and

* Corresponding author. Tel.: +1 713 3486207; fax: +1 713 3485268.
E-mail address: nagaraja@rice.edu (S. Nagarajaiah).

0141-0296/$ - see front matter © 2004 Elsevier Ltd. All rights reserved.
doi:10.1016/j.engstruct.2004.10.015

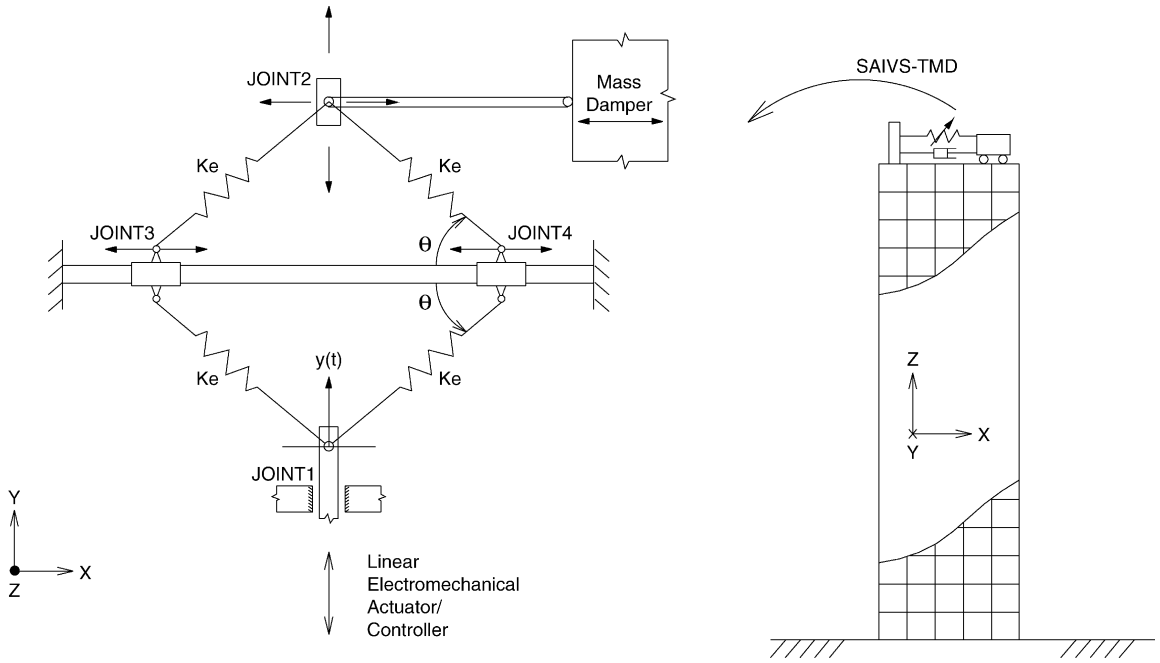

Fig. 1. SAIVS-TMD at the roof level and details of the SAIVS device.

Varadarajan [15,22]. The SAIVS-TMD has a single mass with variable stiffness spring. The system has the distinct advantage of continuously retuning its frequency in real time thus making it robust to changes in building stiffness and damping. In contrast the passive TMD can only be tuned to a fixed frequency. In addition, SAIVS-TMD will behave as a failsafe TMD system; hence, SAIVS-TMD is reliable. It is to be noted that MTMD can overcome some of the limitations of a TMD; however, MTMD cannot be retuned in real time, thus is not adaptable, and space constraints can limit the location of a large number of TMD's.

The effectiveness of the new SAIVS-TMD controlled by the new STFT algorithm for vibration control of a wind excited tall building is evaluated in this study. Frequency tuning of the SAIVS-TMD is achieved by a new time frequency control algorithm based on STFT. Comparisons with a TMD and an ATMD are presented. The effectiveness of SAIVS-TMD with STFT controller in reducing the response, particularly with building stiffness changes, is shown by numerical simulations.

2. Semi-active variable stiffness TMD (SAIVS-TMD)

A new and innovative semi-active variable stiffness (SAIVS) device which can change its stiffness continuously between maximum and minimum stiffness has been developed by Nagarajaiah [14]. As shown in Fig. 1 the SAIVS device consists of four spring elements arranged in a plane rhombus configuration with pivot joints at the vertices. A linear electromechanical actuator reconfigures the aspect ratio of the rhombus configuration of the SAIVS device. The aspect ratio changes between the fully closed (first diagonal between joint 1 and 2 being nearly zero) and open configurations (second diagonal between joint 3 and 4 being nearly zero) producing maximum and minimum stiffness, respectively. STFT control algorithm and controller are used to regulate the electromechanical actuator. The power required to change the aspect ratio of the device is nominal. The variable stiffness of the SAIVS device can be described by the following equation

$$K(t) = k_e \cos^2(\theta(t)) \tag{1}$$

where $K(t)$ is the time varying stiffness of the device, and k_e is the constant spring stiffness of each spring element, $\theta(t)$ is the time varying angle of the spring elements with the horizontal in any position of the device as shown in Fig. 1. The SAIVS device has maximum stiffness in its fully closed position ($\theta(t) = 0$) and minimum stiffness ($\theta(t) \sim \frac{\pi}{2}$) in its fully open position. The device can be positioned in any configuration between closed and open positions; thus, the device is capable of varying the stiffness continuously between the maximum and minimum. The SAIVS device has been tested and shown to be effective by Nagarajaiah and Mate [12]. The SAIVS-TMD has been developed by Nagarajaiah and Varadarajan [15]. The SAIVS-TMD consists of a SAIVS device attached to a mass damper as shown in Fig. 1. In this paper control of SAIVS-TMD using a new STFT algorithm is investigated.

3. Short time Fourier transform algorithm

STFT is a widely used method for studying non-stationary signals [3] as it gives good time–frequency distribution for many signals. To know what frequencies exist at a particular time, consider a small segment of the

signal around that time, and Fourier analyze it neglecting the rest of the signal. Break up the signal into several such segments. Fourier analyse each time segment to ascertain the frequencies that exist in that segment. For each different time a different spectrum is obtained. The totality of these spectra indicates how the spectrum is varying in time and gives the time frequency distribution. Since the time segment or interval is short compared to the whole signal the process is called short time Fourier transform. The time segment is obtained by multiplying the signal $S(\tau)$ by a window function, $h(\tau)$, centered around the time of interest $\tau - t$ to obtain the weighted signal.

$$s_t(\tau) = s(\tau)h(\tau - t). \tag{2}$$

The running time is τ and the fixed time is t. The window function is chosen to leave the signal more or less unaltered around the time, t, but to suppress the signal for times distant from the time of interest. Since the window emphasizes the signal around time, t, the Fourier spectrum will emphasize the frequencies at that time. In particular the spectrum is

$$\begin{aligned} S_t(\omega) &= \frac{1}{\sqrt{2\pi}} \int \mathrm{e}^{-\mathrm{j}\omega\tau} s_t(\tau)\mathrm{d}\tau \\ &= \frac{1}{\sqrt{2\pi}} \int \mathrm{e}^{-\mathrm{j}\omega\tau} s(\tau)h(\tau - t)\mathrm{d}\tau \end{aligned} \tag{3}$$

which is the short time Fourier transform. The energy density of the modified signal (at the fixed time t is)

$$\begin{aligned} P(t,\omega) &= |S_t(\omega)|^2 = |s_\omega(t)|^2 \\ &= \left| \frac{1}{\sqrt{2\pi}} \int \mathrm{e}^{-\mathrm{j}\omega\tau} s(\tau)h(\tau - t)\mathrm{d}\tau \right|^2. \end{aligned} \tag{4}$$

A different spectrum is obtained for each different time and the totality of these spectra gives the time–frequency distribution.

The instantaneous frequency at time t, is given by

$$\langle\omega\rangle_t = \frac{1}{|s(t)|^2} \int \omega |S_t(\omega)|^2 \mathrm{d}\omega. \tag{5}$$

The implementation procedure for the STFT in the discrete domain is carried out by extracting time windows of the original non-stationary signal s. After zero padding and convolving the signal with Hamming window, the DFT is computed for each windowed signal to obtain STFT, S, of signal s. The dominant frequency is obtained from the corresponding Fourier coefficient. If the window width is $n.\Delta t$ (where n is the number of points in the window, and Δt is the sampling rate of the signal), the ith element in S is the Fourier coefficient that corresponds to the frequency

$$\omega_i = i\frac{2\pi}{n.\Delta t} \text{ (for window width } n.\Delta t). \tag{6}$$

4. STFT control algorithm

The stiffness of the SAIVS device is varied continuously based on the STFT control algorithm to tune the SAIVS-TMD. The current dominant frequency of response is identified based on the STFT (Eqs. (2)–(6)) algorithm shown in Figs. 2 and 3. The top floor displacement is the only feedback used in the STFT algorithm. The frequency of the SAIVS-TMD is tuned to the dominant frequency at which the structure is responding to maximize the response reduction. In developing the algorithm the building stiffness uncertainty is assumed to be ±15%. (Any reasonable percentage uncertainty can be assumed in general.)

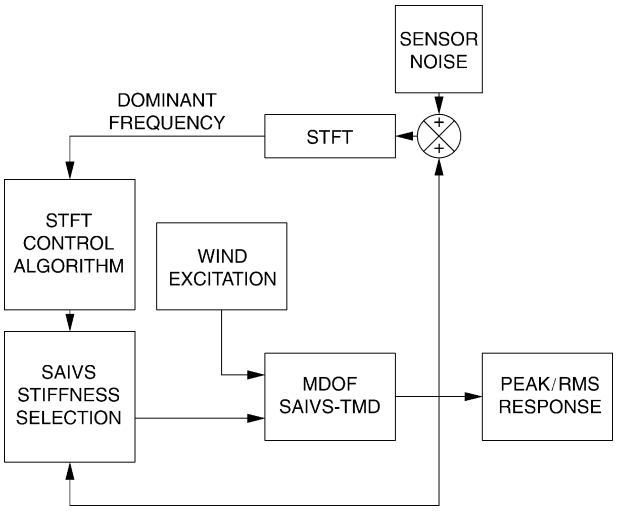

Fig. 2. STFT control algorithm.

The STFT control algorithm developed, shown in Figs. 2 and 3, is as follows:

(1) A moving window of n time steps of signal, is convolved with Hanning window, h, to determine the dominant frequency in the energy spectrum of the top floor displacement at each time step.
(2) STFT is performed on the moving window and the dominant frequency, f_d^i, is identified from the spectrum and compared with fundamental mode frequency in -15% stiffness uncertainty, f_{-15}, and in $+15\%$ stiffness uncertainty, f_{+15}.
(3) If f_d^i lies in the range $f_{-15} < f_d^i < f_{+15}$ then the average frequency, f_{avg}^i, is calculated from the average of f_d^k over m time steps, else f_{avg}^{i-1} of the previous time step is retained as the average for the current time step.
(4) If $f_d^i < 0.95\, f_{avg}^i$ (or $0.95\, f_{avg}^{i-1}$) the SAIVS-TMD frequency is tuned to be equal to $0.95\, f_{avg}^i$ (or $0.95\, f_{avg}^{i-1}$).
(5) If $f_d^i > 1.05\, f_{avg}^i$ (or $1.05\, f_{avg}^{i-1}$) the SAIVS-TMD frequency is tuned to be equal to $1.05\, f_{avg}^i$ (or $1.05.\, f_{avg}^{i-1}$).
(6) If $1.05\, f_{avg}^i > f_d^i > 0.95\, f_{avg}^i$ the SAIVS-TMD is tuned to be equal to f_d^i.

The reason for choosing $0.95\, f_{avg}^i$ and $1.05\, f_{avg}^i$ is because the SAIVS-TMD has the maximum effectiveness in this frequency range, which will be explained further by means of a numerical example. In summary the STFT algorithm identifies the dominant frequency of response, and its

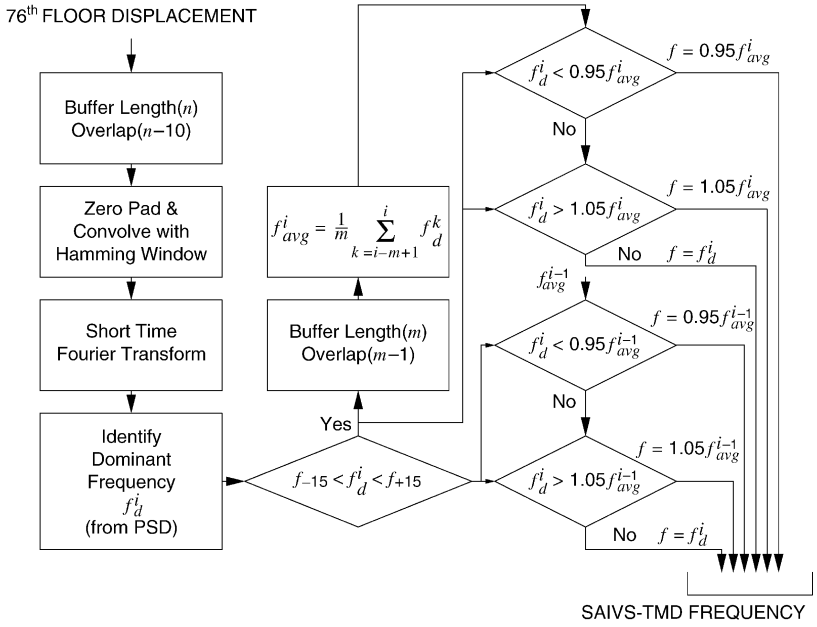

Fig. 3. SAIVS-TMD frequency selection based on STFT algorithm.

variation as a function of time, to retune the SAIVS-TMD in real time.

5. Numerical example

The wind excited tall building by Yang et al. [25,27] is considered as the numerical example. The structural model developed by Yang et al. [25] is that of a 76-story slender building, as shown in Fig. 1, with a single TMD installed above the top floor. The total mass of the building is 153,000 metric tons. The 76 story building was modeled by Yang et al. [25,27] as a vertical cantilever beam, with 76 translational and 76 rotational degrees of freedom (DOF). The 76 rotational DOF were removed by static condensation, retaining the 76 translational DOF. The computed first five natural frequencies of the primary system were 0.16, 0.765, 1.992, 3.790, and 6.395 Hz; the damping ratio of these proportionally damped modes being 1%. The TMD with an inertial mass of 500 tons (0.327% of the total mass of the building) was chosen. Yang et al. [25] chose the undamped natural frequency of the TMD to be 0.16 Hz and a higher than optimal damping ratio of 20% to allow for a bigger stroke for the ATMD. A reduced order model with 23 DOF was chosen to minimize the computational effort; with TMD the model involved 24 DOF.

Wind tunnel tests for a 1:400 scale rigid model of the 76 story building were conducted at Sydney University. For further details about the wind tunnel tests and wind excitation the reader is referred to Yang et al. [25]. The across wind data from the tests are used in the analytical study. Although the wind tunnel data was generated for one hour, a duration of 900 s is used to reduce the computational effort, and such a duration should be sufficient to establish the stationarity properties. The wind forces are lumped at the 24 DOF of the reduced order model.

The analytical model is developed with a linear time invariant primary system and time variant SAIVS-TMD system. The SAIVS-TMD with a mass of 500 tons, similar to the TMD and ATMD, is considered. In order to evaluate the robustness of the controller, the uncertainty in the building stiffness of ±15% is considered. The building fundamental frequency is $f_{+15} = 0.172$ Hz in the +15% case and $f_{-15} = 0.148$ Hz in the −15% case. The frequency of the SAIVS-TMD can vary between f_{-15} to f_{+15}. For the STFT algorithm $n = 2048$ and $m = 200$ are chosen. The damping ratio of the SAIVS-TMD is chosen to be 7%. The first 48 complex modes are used in the model. The state space model of the system is as follows:

$$\dot{\mathbf{X}}(t) = \mathbf{A}(t)\mathbf{X}(t) + \mathbf{E}\mathbf{w}(t) \tag{7}$$

$$\mathbf{y}(t) = \mathbf{C}\mathbf{X}(t) + \nu(t) \tag{8}$$

with $X = (x, \dot{x})$, where x includes the displacements at the reduced order 23 DOF, and x_m, the TMD displacement, all with respect to the ground, $\mathbf{y}(t)$ is the 76th floor displacement. $\mathbf{w}$ is the excitation and ν is the measured noise.

Non-dimensional performance criteria specified [25,27] for comparisons and evaluation of response are as follows. The first criterion is based on the ability to reduce the root mean square (RMS) absolute acceleration:

$$J_1 = \max(\sigma_{\ddot{x}_1}, \sigma_{\ddot{x}_{30}}, \sigma_{\ddot{x}_{50}}, \sigma_{\ddot{x}_{55}}, \sigma_{\ddot{x}_{60}}, \sigma_{\ddot{x}_{65}}, \sigma_{\ddot{x}_{70}}, \sigma_{\ddot{x}_{75}})/\sigma_{\ddot{x}_{75o}} \tag{9}$$

where $\sigma_{\ddot{x}_i}$ is the RMS acceleration of the ith floor, and $\sigma_{\ddot{x}_{75o}}$ is the RMS acceleration of the 75th floor for the uncontrolled case. In the performance criterion J_1, accelerations only up to the 75th floor are considered based on occupant comfort.

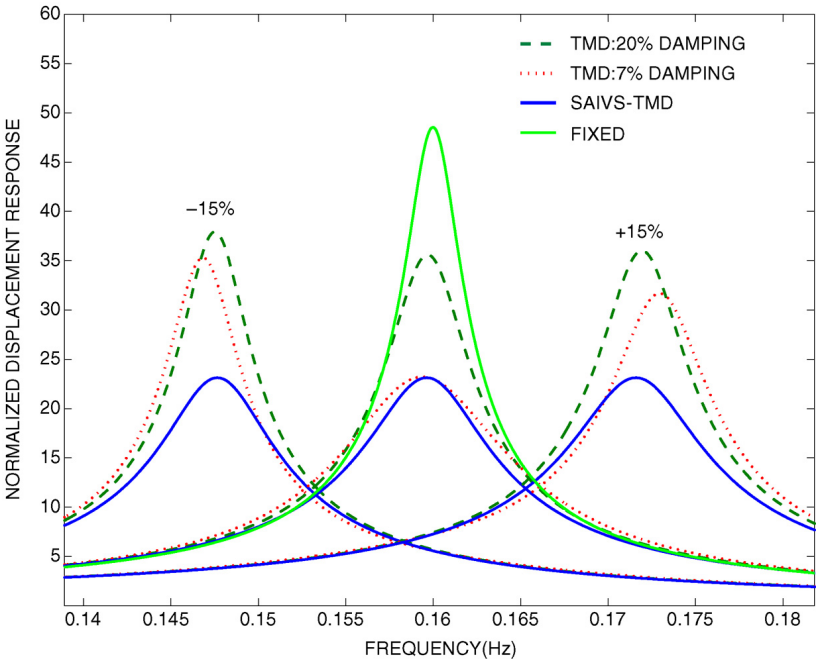

Fig. 4. Top floor displacement frequency response curves for cases with −15%, 0%, 15% stiffness uncertainty and the fixed case.

The second criterion is the average reduction of acceleration for selected floors above the 49th floor

$$J_2 = \frac{1}{6} \sum_{i=50,55,60,65,70,75} \sigma_{\ddot{x}_i} / \sigma_{\ddot{x}_{io}} \tag{10}$$

in which $\sigma_{\ddot{x}_{io}}$ is the RMS acceleration of the ith floor without control. The third and fourth evaluation criteria are the ability of the controllers to reduce the top floor displacements. The normalized form of the two criteria is as follows:

$$J_3 = \sigma_{x_{76}} / \sigma_{x_{76o}} \tag{11}$$

$$J_4 = \frac{1}{7} \sum_{i=50,55,60,65,70,75,76} \sigma_{xi} / \sigma_{x_{io}} \tag{12}$$

where σ_{xi} and $\sigma_{x_{io}}$ are the RMS displacements of the ith floor with and without control, respectively, and $\sigma_{x_{76}}$ and $\sigma_{x_{76o}}$ are the RMS displacement of the 76th floor with and without control, respectively. The control effort requirements are evaluated in terms of the following nondimensional actuator stroke and average power (actuator velocity):

$$J_5 = \frac{\sigma_{xm}}{\sigma_{x_{76o}}} \tag{13}$$

$$J_6 = \frac{\sigma_{\dot{x}_m}}{\sigma_{\dot{x}_{76o}}} \tag{14}$$

where $\sigma_{\dot{x}_m}$ is the RMS actuator velocity (relative velocity between the SAIVS-TMD or ATMD and the top floor) and $\sigma_{\dot{x}_{76o}}$ is the RMS velocity of the 76th floor in the uncontrolled case. For criteria J_7 through J_{10} for peak responses, the RMS response, σ, in criterion J_1 to J_6 is replaced by the peak response, x_p. In addition

$$J_{11} = \frac{x_{pm}}{x_{p_{76o}}} \tag{15}$$

$$J_{12} = P_{\max} = \max_t |\dot{x}_m(t) u(t)| \tag{16}$$

($J_{12} = \dot{x}_{pm}/\dot{x}_{p_{76o}}$ for semi-active devices) represent the peak actuator stroke and peak control power, respectively. For each performance criteria values of less than one mean reductions in response in the case with control when compared to the uncontrolled case. For further details of these criteria, the reader is referred to Yang et al. [25,27].

6. Results

The fixed (no TMD) case, TMD case, and SAIVS-TMD case normalized top floor displacement frequency response curves (normalized with respect to static displacement), considering only the first mode and 1% modal damping, for the cases with 0% and ±15% stiffness uncertainty are shown in Fig. 4. For the wind response computations all modes are considered. The first mode frequency of the primary structure is 0.16, 0.148, and 0.172 Hz for the case with 0% and ±15% stiffness uncertainty, respectively. For 0% damping in the TMD case, the two resonant peaks occur at frequencies ∼0.155 and ∼0.165 Hz. As the damping in the TMD case increases to 7% and 20% a single resonant peak occurs at frequency ∼0.16 Hz as shown in Fig. 4; the corresponding resonant peaks occur at ∼0.148 and ∼0.172 Hz in −15% and +15% stiffness uncertainty case, respectively. The TMD is optimally tuned at 0.16 Hz for 0% stiffness uncertainty and maintained at originally tuned

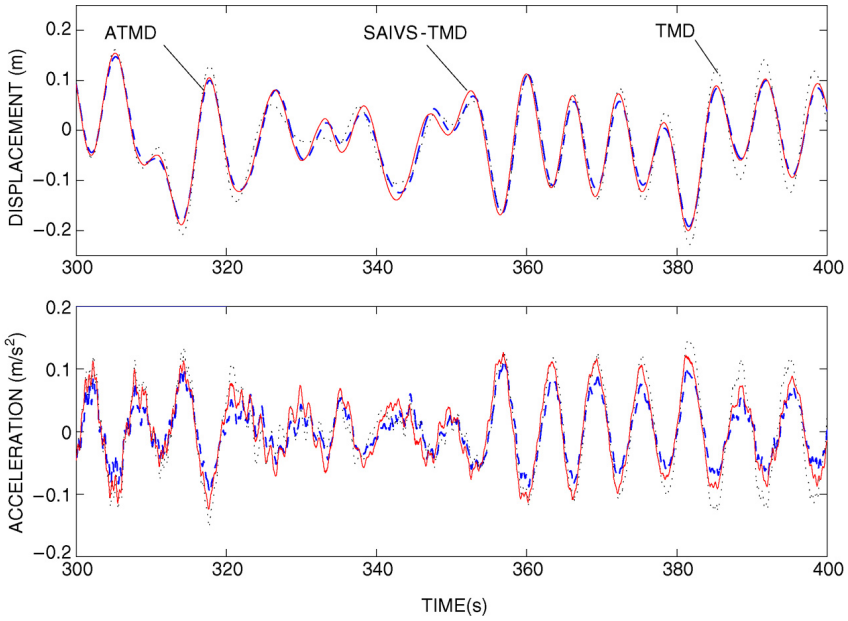

Fig. 5. 75th floor response for TMD, ATMD and SAIVS-TMD case.

0.16 Hz for ±15% stiffness uncertainty. In contrast, the SAIVS-TMD is retuned in the frequency range 0.148 to 0.172 Hz. The reason for choosing $0.95\,f^i_{avg}$ and $1.05\,f^i_{avg}$ in the STFT algorithm is because SAIVS-TMD has the maximum effectiveness in this frequency range. This is evident in the 0% stiffness uncertainty case in Fig. 4 wherein the SAIVS-TMD reduces the response, as compared to the TMD and fixed case, between 0.155 Hz (0.95×0.16 Hz) and 0.165 Hz (1.05×0.16 Hz).

The response reduction, in the case of TMD and SAIVS-TMD with 7% damping, is nearly 57% as compared to the fixed case. In Fig. 4, both TMD and SAIVS-TMD, in the case with 7% damping and 0% stiffness uncertainty, are equally effective in reducing the response; however, this is not so in the TMD case for ±15% stiffness uncertainty, the SAIVS-TMD proves to be much more effective in reducing the response, because of retuning of SAIVS-TMD indicating its robustness capability.

Comparisons between the displacement and acceleration responses of TMD, ATMD and SAIVS-TMD to wind excitation for 0% uncertainty are shown in Fig. 5. The responses of the TMD computed and presented in this study are identical to that of Yang et al. [25]. The ATMD is controlled by a LQG controller developed by Yang et al. [25] and the results presented are from this study. The responses of the SAIVS-TMD and ATMD are comparable and are less than the response of the TMD.

The STFT spectrogram and the 76th floor response are shown in Figs. 6 and 7. It is evident from Figs. 6 and 7 that the STFT algorithm identifies the dominant frequency of response. The frequency variation of SAIVS-TMD is overlaid on the spectrogram in Fig. 7 to indicate its correlation with the dominant frequency identified by STFT algorithm.

The force–displacement response of the TMD spring and SAIVS device of the SAIVS-TMD are shown in Fig. 8. The stiffness variation, evident in Fig. 8, in the case of SAIVS-TMD, tunes the frequency continuously to achieve maximum reduction in response, whereas, the stiffness of the TMD remains fixed.

The 75th floor acceleration power spectral density for TMD, SAIVS-TMD, and ATMD are shown in Fig. 9; it is clearly evident that SAIVS-TMD reduces the response further to TMD. Also, in Fig. 9, the SAIVS-TMD reduces the response in the first mode and, reduces the response in the higher modes also.

Detailed peak and RMS responses are presented in Tables 1 through 5. Table 1 compares the peak displacement and acceleration responses of the uncontrolled structure, the structure with TMD, the structure with SAIVS-TMD, and the structure with ATMD, in the case with 0% stiffness uncertainty. The TMD reduces the 76th floor displacement and acceleration response by nearly 20% and 35% respectively, when compared to the uncontrolled case. From Table 1 it is evident that the SAIVS-TMD reduces the peak displacement and acceleration response of the 76th floor by nearly 30% and 55%, respectively, when compared to the uncontrolled case; corresponding reductions in the case of ATMD are nearly 30% and 50%, respectively. Further reduction in the case of SAIVS-TMD, when compared to the TMD case, is 9% response reduction in displacement and 31% response reduction in acceleration; the corresponding reductions in the case of ATMD are 9% and 23%. Hence, it is evident that SAIVS-TMD is as effective as ATMD in reducing the response. SAIVS-TMD

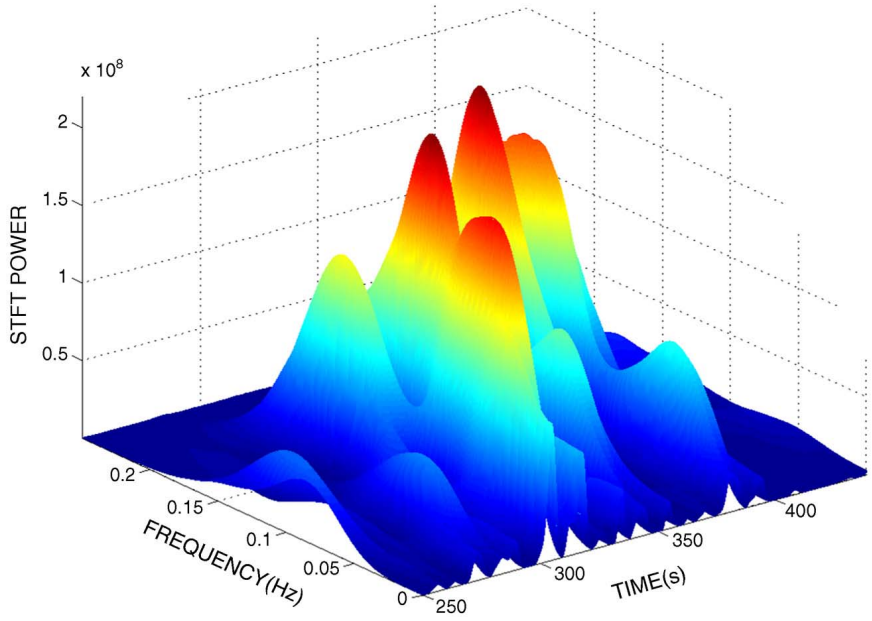

Fig. 6. Spectrogram of 76th floor displacement.

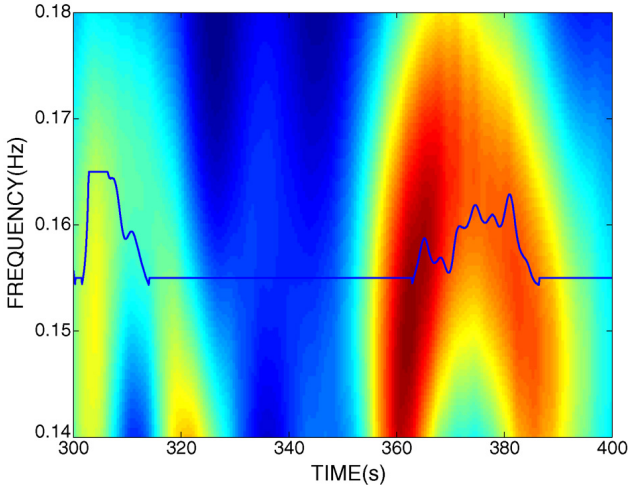

Fig. 7. Time–frequency distribution overlaid with frequency variation of SAIVS-TMD, varying between 0.155 and 0.165 Hz.

is more effective than the TMD—even though the TMD is tuned in the case with 0% stiffness uncertainty—because it continuously retunes the frequency effectively.

In Table 2, the RMS displacement and acceleration responses are compared for the same cases. The reductions in the 76th floor displacement and acceleration RMS response are nearly 40% to 50%, in the case of SAIVS-TMD, when compared to the uncontrolled or fixed case; similar reductions are observed in the case of ATMD also. In the case of SAIVS-TMD the 76th floor displacement and acceleration responses are further reduced from the TMD case by 12% and 21%, respectively.

The performance criteria J_1 through J_{12} for SAIVS-TMD and ATMD cases for stiffness uncertainty, $\Delta K = 0\%$, and $\pm 15\%$, are presented in Table 3. Similar performances in the SAIVS-TMD and ATMD cases are evident in Table 3. Nearly 40% to 55% reduction occurs in the RMS acceleration criteria, J_1 and J_2, peak acceleration criteria, J_7 and J_8. The reduction in the RMS displacement criteria, J_3 and J_4, peak displacement criteria, J_9 and J_{10} varies from 16% to 49%. The performance in the case of SAIVS-TMD is nearly the same as the ATMD. However, the important difference, in the case of SAIVS-TMD, is J_6—the average power consumption—is significantly smaller, and J_{12}—the peak power consumption—is an order of magnitude smaller, when compared to the ATMD. Fully active systems need substantial power since they apply active forces on to the TMD. However, the SAIVS-TMD achieves the response reduction by continuously varying the stiffness and retuning the frequency and not by application of active forces, thus the semi-active case needs nominal power. Also, in the event of power failure SAIVS-TMD can readily act as a TMD.

The peak displacement and acceleration responses for uncontrolled, TMD, ATMD, and SAIVS-TMD cases for stiffness uncertainty of $+15\%$ are presented in Table 4. The TMD reduces the 76th floor displacement and acceleration response by nearly 21% and 22%, respectively, when compared to the uncontrolled or fixed case; the corresponding reductions in the case of SAIVS-TMD and ATMD are nearly 22% and 27% respectively. The displacement and acceleration response of the ATMD and SAIVS-TMD cases are within a few percent of each other and are equally effective in reducing the response as compared to the uncontrolled or fixed case. It should be kept in mind that SAIVS-TMD power requirements are substantially lower than those of the ATMD.

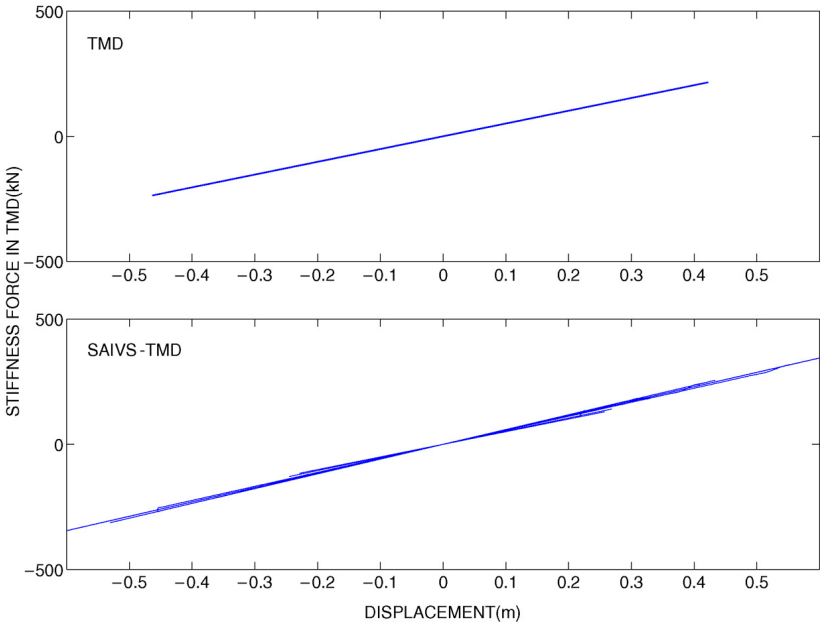

Fig. 8. Force–displacement behavior: (a) TMD spring; (b) SAIVS-TMD variable stiffness spring.

Table 1
Comparison of peak response for 0% uncertainty in stiffness

Floor no.	Uncontrolled		TMD		ATMD[a]		SAIVS-TMD	
	x_{pio} (cm)	$\ddot{x}_{pio}$ (cm/s^2)	x_{pi} (cm)	$\ddot{x}_{pi}$ (cm/s^2)	x_{pi} (cm)	$\ddot{x}_{pio}$ (cm/s^2)	x_{pi} (cm)	$\ddot{x}_{pio}$ (cm/s^2)
1	0.05	0.22	0.04	0.21	0.04	0.23	0.04	0.27
30	6.84	7.14	5.60	4.68	5.14	3.37	5.09	3.56
50	16.59	14.96	13.34	9.28	12.22	6.73	12.10	7.38
55	19.41	17.48	15.54	10.74	14.22	8.05	14.09	8.01
60	22.34	19.95	17.80	12.69	16.27	8.93	16.13	9.08
65	25.35	22.58	20.10	14.72	18.36	10.05	18.20	10.40
70	28.41	26.04	22.43	16.77	20.48	10.67	20.30	11.50
75	31.59	30.33	24.84	19.79	22.67	11.56	22.48	13.74
76	32.30	31.17	25.38	20.52	23.15	15.89	22.96	14.15
Md	–	–	42.36	46.18	74.27	72.74	69.62	70.97

[a] The response of ATMD from [25].

Table 2
Comparison of RMS response for 0% uncertainty in stiffness

Floor no.	Uncontrolled		TMD		ATMD[a]		SAIVS-TMD	
	σ_{pio} (cm)	$\ddot{\sigma}_{pio}$ (cm/s^2)	σ_{pi} (cm)	$\ddot{\sigma}_{pi}$ (cm/s^2)	σ_{pi} (cm)	$\ddot{\sigma}_{pio}$ (cm/s^2)	σ_{pi} (cm)	$\ddot{\sigma}_{pio}$ (cm/s^2)
1	0.02	0.06	0.01	0.06	0.01	0.06	0.01	0.06
30	2.15	2.02	1.48	1.23	1.26	0.89	1.30	0.99
50	5.22	4.78	3.57	2.80	3.04	2.03	3.13	2.20
55	6.11	5.59	4.17	3.26	3.55	2.41	3.66	2.56
60	7.02	6.42	4.79	3.72	4.08	2.81	4.21	2.93
65	7.97	7.31	5.43	4.25	4.62	3.16	4.77	3.35
70	8.92	8.18	6.08	4.76	5.17	3.38	5.33	3.75
75	9.92	9.14	6.75	5.38	5.74	3.34	5.92	4.27
76	10.14	9.35	6.90	5.48	5.86	4.70	6.05	4.35
Md	–	–	12.76	13.86	23.03	22.40	22.32	22.76

[a] The response of ATMD from [25].

Table 3
Comparison of performance criteria

RMS responses SAIVS-TMD (ATMD LQG controller)[a]				Peak responses SAIVS-TMD (ATMD LQG controller)[a]			
Criteria	$\Delta K = 0\%$	$\Delta K = 15\%$	$\Delta K = -15\%$	Criteria	$\Delta K = 0\%$	$\Delta K = 15\%$	$\Delta K = -15\%$
J_1	0.467 (0.369)	0.459 (0.365)	0.498 (0.387)	J_7	0.453 (0.381)	0.498 (0.411)	0.566 (0.488)
J_2	0.460 (0.417)	0.446 (0.409)	0.498 (0.438)	J_8	0.460 (0.432)	0.472 (0.443)	0.571 (0.539)
J_3	0.597 (0.578)	0.506 (0.487)	0.741 (0.711)	J_9	0.711 (0.717)	0.615 (0.607)	0.840 (0.770)
J_4	0.598 (0.580)	0.508 (0.489)	0.743 (0.712)	J_{10}	0.719 (0.725)	0.620 (0.614)	0.848 (0.779)
J_5	2.201 (2.271)	1.767 (1.812)	2.462 (2.709)	J_{11}	2.156 (2.300)	1.795 (1.852)	2.610 (2.836)
J_6	2.378 (11.99)	2.054 (8.463)	2.486 (16.61)	J_{12}	2.256 (71.87)	2.082 (52.68)	2.654 (118.33)

[a] The response of ATMD from [25].

Table 4
Comparison of peak response for +15% uncertainty in stiffness

Floor no.	Uncontrolled		TMD		ATMD[a]		SAIVS-TMD	
	x_{pio} (cm)	$\ddot{x}_{pio}$ (cm/s^2)	x_{pi} (cm)	$\ddot{x}_{pi}$ (cm/s^2)	x_{pi} (cm)	$\ddot{x}_{pio}$ (cm/s^2)	x_{pi} (cm)	$\ddot{x}_{pio}$ (cm/s^2)
1	0.04	0.22	0.03	0.22	0.03	0.23	0.035	0.30
30	5.52	4.78	4.40	4.38	4.35	3.36	4.39	3.97
50	13.37	11.28	10.65	8.16	10.35	6.63	10.43	7.10
55	15.63	12.85	12.43	9.67	12.04	8.00	12.14	8.06
60	17.94	14.91	14.27	11.18	13.78	9.13	13.89	9.03
65	20.32	16.87	16.15	12.79	15.55	10.09	15.68	10.31
70	22.72	18.98	18.05	14.57	17.34	11.58	17.49	12.65
75	25.20	21.75	20.01	16.86	19.19	12.46	19.44	15.11
76	25.76	21.60	20.45	16.84	19.60	15.86	19.87	15.55
Md	–	–	32.61	35.73	59.83	60.87	57.99	59.23

[a] The response of ATMD from [25].

Table 5
Comparison of peak response for −15% uncertainty in stiffness

Floor no.	Uncontrolled		TMD		ATMD[a]		SAIVS-TMD	
	x_{pio} (cm)	$\ddot{x}_{pio}$ (cm/s^2)	x_{pi} (cm)	$\ddot{x}_{pi}$ (cm/s^2)	x_{pi} (cm)	$\ddot{x}_{pio}$ (cm/s^2)	x_{pi} (cm)	$\ddot{x}_{pio}$ (cm/s^2)
1	0.06	0.22	0.06	0.21	0.04	0.22	0.047	0.31
30	7.69	6.01	7.91	5.08	5.54	3.64	6.00	4.11
50	18.34	12.83	16.92	10.93	13.12	7.87	14.25	8.47
55	21.37	14.41	19.72	12.26	15.27	9.90	16.60	10.12
60	24.49	15.97	22.59	13.63	17.47	11.13	19.01	11.22
65	27.68	17.40	25.53	15.39	19.72	12.63	21.48	13.03
70	30.90	19.86	28.50	17.95	21.99	14.01	23.98	14.92
75	34.24	23.09	31.58	21.08	24.34	14.80	26.56	17.16
76	34.99	22.80	32.27	20.73	24.87	18.76	27.14	17.16
Md	–	–	44.93	48.65	91.60	79.06	84.29	85.88

[a] The response of ATMD from [25].

The peak displacement and acceleration responses for uncontrolled, TMD, ATMD, and SAIVS-TMD cases for stiffness uncertainty values of −15% are presented in Table 5. The displacement and acceleration response for the

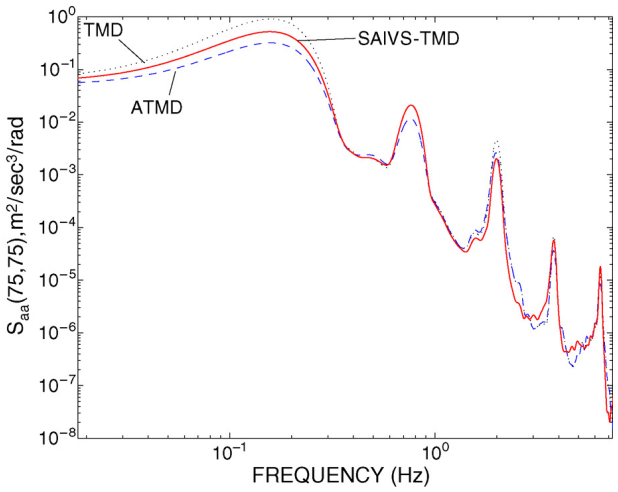

Fig. 9. Power spectral distribution of 75th story acceleration.

case of TMD is within 10% of the uncontrolled case and clearly the effectiveness of the TMD is diminished since it is mistuned. However, the SAIVS-TMD is still effective as it can retune and reduce the response by nearly 20% to 25% when compared to the uncontrolled case, and by 15% when compared to the TMD case. The responses of the SAIVS-TMD and the ATMD are within a few percent of each other; it should be kept in mind that SAIVS-TMD power requirements are substantially lower than those of the ATMD. Hence, the SAIVS-TMD is effective in all cases, i.e., 0% and ±15% stiffness uncertainty, similar to an ATMD.

7. Conclusions

Semi-active variable stiffness TMD for wind response control of tall buildings has been studied analytically using the developed STFT algorithm. The STFT algorithm is effective in retuning the stiffness of SAIVS-TMD and in reducing the response to wind excitation. The SAIVS-TMD is robust and effective in reducing the response of tall structures, particularly in cases with stiffness uncertainty of ±15% or more. The TMD loses its effectiveness with ±15% stiffness variation. The performance of the SAIVS-TMD with STFT algorithm is similar to that of an ATMD, but with an order of magnitude less power consumption. SAIVS-TMD is specially suited for cases where the buildings exhibit nonlinearity resulting in amplitude dependence of natural frequencies. If the amplitude dependency of the natural frequency is known from vibration records of the buildings under various levels of wind excitation, then the stiffness adjustments can be performed off-line, in which case, real time instantaneous frequency tracking would not be needed; the SAIVS-TMD would essentially be an adjustable passive TMD. This study also shows that algorithms based on time–frequency methods, such as STFT hold significant promise for identification and control of variable stiffness systems.

Acknowledgement

Funding for this project provided by the National Science Foundation, NSF Career Grant CMS-9996244 is gratefully acknowledged.

References

[1] Abe M, Igusa T. Semi-active dynamic vibration absorbers for controlling transient response. J Sound Vibration 1996;198(5): 547–69.
[2] Chang JCH, Soong TT. Structural control using active tuned mass dampers. J Engrg Mech, ASCE 1980;106(6):1091–8.
[3] Cohen L. Time–frequency analysis. 1st ed. NJ: Prentice-Hall; 1995.
[4] Den Hartog JP. Mechanical vibrations. NY: McGraw Hill; 1947.
[5] Gavin H. Design method for high-force electrorheological dampers. Smart Mater Struct 1998;7:664–73.
[6] Hrovat D, Barak P, Rabins M. Semiactive versus passive or active tuned mass dampers for structural control. J Engrg Mech, ASCE 1982; 109(3):691–705.
[7] Igusa T, Xu K. Dynamic characteristics of multiple tuned mass substructures with closed spaced frequencies. Earthquake Engrg Struct Dyn 1992;21:1050–70.
[8] Jabbari F, Bobrow J. Vibration suppression with resettable device. J Engrg Mech, ASCE 2002;128(9):916–24.
[9] Ikeda Y, Sasaki K, Sakamoto M, Kobori T. Active mass driver system as the first application of active structural control. Earthquake Engrg Struct Dyn 2001;30(11):1575–95.
[10] Kobori T, Takahashi M. Seismic response controlled structure with active variable stiffness system. Earthquake Engrg Struct Dyn 1993; 22(12):925–41.
[11] Kurata N, Kobori T, Takahashi M, Niwa N, Midorikawa H. Actual seismic response controlled building with semiactive damper system. Earthquake Engrg Struct Dyn 1999;28:1427–47.
[12] Nagarajaiah S, Mate D. Semi-active control of continuously variable stiffness system, In: Proc sec world conf struct control, vol. 1. 1998. p. 397–405.
[13] Nagarajaiah S, Nadathur V, Sahasrabudhe S. Variable stiffness and instantaneous frequency. In: Proceedings world structures congress'99. New Orleans (LA): ASCE; 1999. p. 281–92.
[14] Nagarajaiah S. Structural vibration damper with continuously variable stiffness. US Patent No. 6,098,969, August 8; 2000.
[15] Nagarajaiah S, Varadarajan N. Novel semi-active variable stiffness tuned mass damper with real time tuning capability. In: Proc. 13 eng mech conf, ASCE, UT-Austin, CD ROM; 2000.
[16] Reinhorn A, Soong TT, Riley MA, Lin RC, Aizawa S, Higashino M. Full sale implementation of active control. II: installation and performance. J Struct Engrg, ASCE 1993;119(6):1935–60.
[17] Soong TT. Active structural control: theory and practice. NY: Longman Scientific Tech.; 1990.
[18] Spencer BF, Dyke SJ, Sain MK, Carlson JD. Phenomenological model for MR dampers. J Engrg Mech, ASCE 1997;123(3):230–8.
[19] Spencer BF, Nagarajaiah S. State of the art of structural control. J Struct Engrg, ASCE 2003;129(7):1–10.
[20] Symans M, Constantinou MC. Seismic testing of a building structure with a semi-acive fluid damper control system. Earthquake Engrg Struct Dyn 1999;26(7): 21,759–77.
[21] Sun JQ, Jolly MR, Norris MA. Passive, adaptive, and active tuned vibration absorbers: a survey. J Vib Acoustics and J Mech Design 1995;117(B):234–42. 50th Anniversary Issue of ASME.
[22] Varadarajan N, Nagarajaiah S. Wind response control of building with variable stiffness TMD: EMD/HT. J Eng Mech, ASCE 2004;130(4) [in press].
[23] Warburton GB. Optimum absorber parameters for minimizing vibration response. Earthquake Engrg Struct Dyn 1981;9:251–62.

[24] Yalla SK, Kareem A, Kantor JC. Semi-active tuned liquid dampers for vibration control of structures. Engrg Struct 2001;23: 1469–79.
[25] Yang JN, Agrawal A, Samali B, Wu JC. A benchmark problem for response control of wind excited tall buildings. In: Proc. of 14th eng. mech. conf., ASCE, UT-Austin, CD ROM; 2000.
[26] Yang JN, Kim JH, Agrawal A. Resetting semiactive stiffness damper for seismic response control. J Struct Engrg, ASCE 2000;126(12): 1427–33.
[27] Yang JN, Agrawal A, Samali B, Wu JC. A benchmark problem for response control of wind excited tall buildings. J Engrg Mech, ASCE 2004;130(4) 437–46.